



Bilateral renal histiocytic sarcoma with disseminated lung involvement in a Siberian Forest Cat

Authors: Salord Torres, Xavier, Dobromylskyj, Melanie, Sánchez Jiménez, César, Plested, Mark, Purzycka, Katarzyna, et al.

Source: Journal of Feline Medicine and Surgery Open Reports, 9(2)

Published By: SAGE Publishing

URL: <https://doi.org/10.1177/20551169231191076>

BioOne Complete (complete.BioOne.org) is a full-text database of 200 subscribed and open-access titles in the biological, ecological, and environmental sciences published by nonprofit societies, associations, museums, institutions, and presses.


Your use of this PDF, the BioOne Complete website, and all posted and associated content indicates your acceptance of BioOne's Terms of Use, available at www.bioone.org/terms-of-use.

Usage of BioOne Complete content is strictly limited to personal, educational, and non - commercial use. Commercial inquiries or rights and permissions requests should be directed to the individual publisher as copyright holder.

BioOne sees sustainable scholarly publishing as an inherently collaborative enterprise connecting authors, nonprofit publishers, academic institutions, research libraries, and research funders in the common goal of maximizing access to critical research.



Bilateral renal histiocytic sarcoma with disseminated lung involvement in a Siberian Forest Cat

Xavier Salord Torres¹ , Melanie Dobromylskyj², César Sánchez Jiménez¹, Mark Plested¹, Katarzyna Purzycka¹, Matthew Phillips³ and Deirdre Mallowney¹

Journal of Feline Medicine and Surgery Open Reports
1–7

© The Author(s) 2023

Article reuse guidelines:

sagepub.com/journals-permissions

DOI: 10.1177/20551169231191076

journals.sagepub.com/home/jfmsopenreports

This paper was handled and processed by the European Editorial Office (ISFM) for publication in *JFMS Open Reports*



Abstract

Case summary A 5-year-old female neutered Siberian Forest Cat presented with a 7-day history of lethargy, hyporexia and weight loss. Abdominal ultrasonography revealed bilateral renal changes suggestive of neoplasia. Thoracic radiography documented diffuse pulmonary nodules. The cat was euthanased during diagnostic investigations. Histopathological assessment and immunohistochemical staining of post-mortem renal biopsies were consistent with a histiocytic lesion, most likely histiocytic sarcoma (HS). The lung lesions were suspected of representing disseminated disease.

Relevance and novel information HS is considered a rare neoplastic process in cats. This report describes a case of feline bilateral renal HS with suspected concomitant pulmonary involvement. A primary renal origin was suspected, with the lung lesions being a result of disseminated disease. Renal HS should be included as a differential diagnosis when renal ultrasonography reveals changes suggestive of neoplasia.

Keywords: Histiocytic; sarcoma; renal; disseminated; neoplasia; kidney

Accepted: 13 July 2023

Case description

A 5-year-old female neutered Siberian Forest Cat presented to a referral hospital with a 7-day history of lethargy, inappetence and weight loss. Before referral, the cat had been seen at a primary care practice and received a 2-day course of amoxicillin/clavulanate. Previous medical history was unremarkable. Preventive healthcare was up to date.

On presentation, the cat was quiet, alert and responsive, with pale/pink mucous membranes, moderate dental disease and ptyalism. Its heart rate was 200 beats per minute and respiratory rate was 36 breaths per minute. Rectal temperature was high-normal (39.2°C). The cat was tense on abdominal palpation, but it remained uncertain whether this was a response to pain or stress. Body condition was poor (score 2/9) with generalised severe muscle wastage. The owner reported relatively acute weight loss, but a more chronic weight loss was also deemed possible.

Complete blood count, serum biochemistry and urinalysis documented several abnormalities (Table 1). Feline retrovirus screening (SNAP Combo Plus FeLV/FIV; IDEXX) was negative.

The cat was sedated with intravenous dexmedetomidine (Dexdomitor; Vetoquinol UK) at 10 µg/kg, and butorphanol (Torbugesic; Zoetis UK) at 0.3 mg/kg. Abdominal ultrasonography documented bilaterally enlarged kidneys (up to 4.5 cm long) of an irregular

¹Lumbry Park Veterinary Specialists (CVS Group), Alton, Hampshire, UK

²FINN Pathologists, Norfolk, UK

³Veterinary Pathology Group (VPG), Exeter, UK

Corresponding author:

Xavier Salord Torres DVM, MRCVS, Lumbry Park Veterinary Specialists, Selborne Road, Alton, Hampshire GU34 3HL, UK
Email: xaviersalord@gmail.com



Creative Commons Non Commercial CC BY-NC: This article is distributed under the terms of the Creative Commons

Attribution-NonCommercial 4.0 License (<https://creativecommons.org/licenses/by-nc/4.0/>) which permits non-commercial use, reproduction and distribution of the work without further permission provided the original work is attributed as specified on the SAGE and Open Access pages (<https://us.sagepub.com/en-us/nam/open-access-at-sage>).

Table 1 Complete blood count, serum biochemistry and urinalysis results

Parameter (unit)	Result	RI
Complete blood count		
WBC ($\times 10^9/l$)	44.2*	4.0–15.0
RBC ($\times 10^{12}/l$)	4.47*	5.50–10.00
Haemoglobin (g/dl)	6.9*	8.0–15.0
PCV (%)	24.0*	27.0–50.0
Absolute reticulocyte count ($\times 10^9/l$)	35	<60 non-regenerative (or pre-regenerative) 60–120 mild regeneration 120–220 moderate regeneration >220 marked regeneration
Platelets ($\times 10^9/l$)	218	200–600
Neutrophils ($\times 10^9/l$)	36.7*	2.5–12.5
Band neutrophils ($\times 10^9/l$)	0.4*	0.0–0.3
Lymphocytes ($\times 10^9/l$)	4.4	1.5–7.0
Monocytes ($\times 10^9/l$)	0.9*	0.0–0.8
Eosinophils ($\times 10^9/l$)	1.8*	0.0–1.5
Basophils	0.0	NA
Blood film evaluation	Few neutrophils show slight toxicity No atypical WBC seen	
Serum biochemistry		
Total protein (g/l)	67.6	56.0–81.0
Albumin (g/l)	29.6	26.0–42.0
Total globulin (g/l)	38.0	15.0–57.0
Urea (mmol/l)	9.5	6.1–12.5
Creatinine ($\mu\text{mol/l}$)	128	45–170
Bile acids ($\mu\text{mol/l}$)	2.9	0.0–15.0
Total bilirubin ($\mu\text{mol/l}$)	5.7	0.0–10.0
ALP (U/l)	5*	11–67
ALT (U/l)	22	18–77
AST (U/l)	39	0.1–69
GGT (U/l)	<5	0.1–9.0
GLDH (U/l)	<1	0.0–10.0
Sodium (mmol/l)	155	140–157
Potassium (mmol/l)	4.09	3.40–5.60
Chloride (mmol/l)	120	111–129
CK (U/l)	608*	0–360
Calcium (mmol/l)	2.30	1.60–3.00
Phosphate (mmol/l)	2.03	0.70–2.10
Cholesterol (mmol/l)	3.8	0.9–6.5
Triglycerides (mmol/l)	0.53	0.20–1.30
Glucose (mmol/l)	8.0*	3.8–7.6
Vitamin B12 (pmol/l)	542*	220–500
Folate (nmol/l)	13.6*	19.0–37.0
fPL ($\mu\text{g/l}$)	1.9	0.1–3.5
DGGR lipase (U/l)	12	0–25
TLI (ng/ml)	62	35–130
Urinalysis (cystocentesis sample)		
UPC	0.85*	<0.4
Urine appearance	Yellow, slightly turbid	NA
USG	1.042	NA
pH	7.0	NA

(Continued)

Table 1 (Continued)

Urinalysis (cystocentesis sample)		
Glucose/ketones/bilirubin	Negative	NA
Haemoglobin	+++	NA
WBC (cells/ μ l)	0	NA
RBC (cells/ μ l)	307	NA
Squamous epithelia (cells/ μ l)	0	NA
Bacteria/crystals/casts	Not seen	NA
Culture	Negative	NA

*Abnormal value

ALP = alkaline phosphatase; ALT = alanine transaminase; AST = aspartate transaminase; CK = creatine kinase; DGGR = 1,2-o-dilauryl-rac-glycero-3-glutaric acid-(6'-methylresorufin) ester; fPL = feline pancreas-specific lipase; GGT = gamma-glutamyl transferase; GLDH = glutamate dehydrogenase; MCH = mean cell haemoglobin; MCHC = mean cell haemoglobin concentration; MCV = mean cell volume; NA = not applicable; PCV = packed cell volume; RBC = red blood cells; RI = reference interval; TLI = trypsin-like immunoreactivity; UPC = urine protein:creatinine ratio; USG = urine specific gravity; WBC = white blood cells

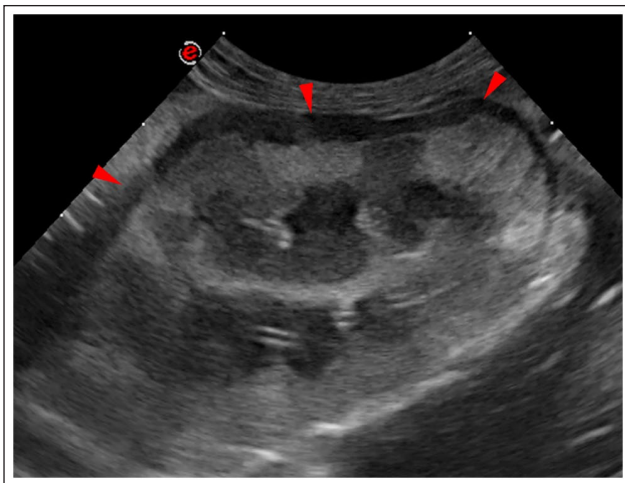


Figure 1 Hyperechoic and enlarged left kidney with hyperechoic renal cortex and well-differentiated and generalised hypoechoic thick rim in the subcapsular space (red arrowheads)

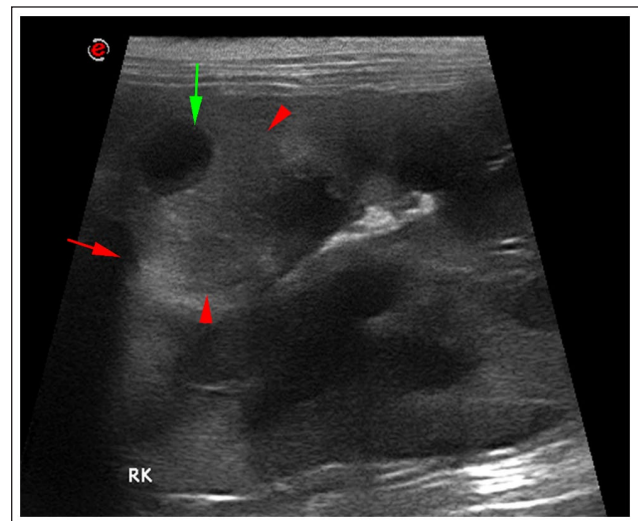


Figure 2 Hyperechoic and enlarged right kidney with an isoechoic nodule (between arrowheads) with a hypo- to anechoic area arising from the renal cortex (green arrow) and modifying the normal shape of the renal capsule (red arrow)

distorted shape. Both kidneys had heterogeneous cortical echogenicity, a thick subcapsular hypoechoic rim (Figure 1) and at least three bulging cortical nodules measuring 1–5 mm with hypoechoic areas (one in the left kidney and two in the right kidney) (Figure 2). No pyelectasia was documented but a small-volume retroperitoneal effusion was present. These features were consistent with bilateral renal neoplasia, with lymphoma considered most likely. Bilateral renal adenocarcinoma or other non-neoplastic differentials, such as bilateral severe nephritis with abscessation, while unlikely given the similarity of the findings to renal lymphoma, could not be completely excluded. Ultrasound-guided fine-needle aspirations (USFNA) of the renal cortices and subcapsular rim were obtained for cytology; air-dried slides were prepared and stained with Modified Wright's stain. Slides were examined by a resident in clinical pathology (M Phillips) and supervised by a board-certified veterinary clinical pathologist.

Cytology demonstrated a very high number of atypical cells consistent with malignant neoplasia, but which were very poorly differentiated and challenging to classify; they were polygonal, ranging from round to caudate, and contained moderate to large quantities of pale basophilic cytoplasm often containing a low number of fine punctate vacuoles. Nuclear to cytoplasmic ratio was moderate and nuclei were often eccentric, oval to polygonal, with reticular chromatin and often one large distinct nucleolus. Frequent binucleate and occasional multinucleate cells were observed; some displayed erythrophagia and leukophagia. Occasional mitotic figures were also seen. Individually, the cells had features suggestive of histiocytic origin and therefore of histiocytic sarcoma (HS); in other areas, the cells appeared more cohesive, a feature more consistent with epithelial origin. In addition, cytology revealed moderate pyogranulomatous inflammation.

Thoracic radiography (dorsoventral, right lateral and left lateral views) documented a moderate number of poorly to moderately well-defined soft-tissue nodules, round to slightly irregular in shape and up to 4 mm in diameter peripherally through all lung lobes (Figure 3). In addition, there was a moderate generalised bronchial pattern.

Given the high suspicion of disseminated neoplasia, and guarded long-term prognosis, the client made the decision to euthanase the cat. Euthanasia was performed 24 h after investigations when the cytology results became available. Meanwhile, the cat remained hospitalised and received maintenance fluid therapy with Ringer's lactate solution (Vetivex 11 solution for infusion; Dechra Veterinary Products), maropitant (Prevomax; Dechra Veterinary Products) at 1 mg/kg IV q24h, mirtazapine (Summit Veterinary Pharmaceuticals) at 2 mg (total dose) PO q24h and buprenorphine (Buprecare; Animalcare) at 0.02 mg/kg IV q6h. Owner consent was obtained for post-mortem sampling.

Ultrasound-guided Tru-cut biopsies (Surgitvet 14G 9-cm vet core biopsy needle) were collected from each kidney, which were fixed in 10% neutral buffered formalin. Each tissue sample was processed and embedded into paraffin blocks, from which 4- μ m-thick sections were stained with haematoxylin and eosin and examined by a board-certified veterinary pathologist (MD). Histopathological evaluation confirmed neoplastic cells very similar in appearance at both sites. For the sample from the right kidney, the neoplastic cells were infiltrating between and separating pre-existing renal tubules, in places completely effacing normal tissue structures (no normal renal tissue was present in the sample from the left kidney); elsewhere, neoplastic cells were arranged in sheets, indistinct clusters or aggregates. Neoplastic cells were also associated with variable numbers of neutrophils, reactive fibroblasts and areas of haemorrhage with possible necrosis. These cells were variable in size and shape; generally, they were medium to large and polygonal, angular or occasionally elongated, with small to moderate amounts of cytoplasm and variably distinct cell borders. Their nuclei were medium to large, paracentral to eccentric and ovoid to irregular in shape, with small amounts of moderately stippled to clumped chromatin and one or two sometimes large and prominent nucleoli (Figure 4). There was moderate to marked anisokaryosis and anisocytosis, with 0–2 mitotic figures seen per high-power field (400 \times ; 0.237 mm²).

The histopathological findings confirmed the cytological results, with an appearance and growth pattern most suggestive of HS (Figure 4). A poorly differentiated carcinoma was considered a less likely differential diagnosis. Immunohistochemical staining was performed; the neoplastic cell population demonstrated strong positive cytoplasmic staining for the mesenchymal cell



Figure 3 Left lateral radiograph of the thorax. Multiple small, ill-defined, soft-tissue nodules are scattered throughout the pulmonary parenchyma. The rest of the thoracic structures are unremarkable

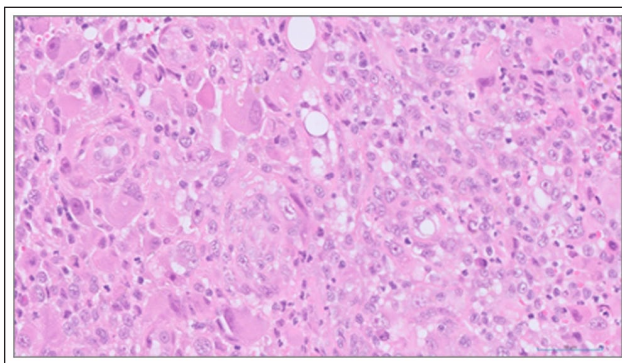


Figure 4 Histological section from a post-mortem Tru-cut biopsy obtained from the right kidney. Variably sized, polygonal, angular to elongated neoplastic cells can be seen, arranged in sheets or indistinct clusters, admixed with low numbers of inflammatory cells. Neoplastic cells have moderate to sometimes large amounts of cytoplasm, variably distinct cell borders and one or two variably sized, sometimes large, round to ovoid nuclei, with often large and prominent nucleoli. Haematoxylin and eosin, 100 \times magnification

marker vimentin (Figure 5) and was negative for the epithelial cell marker cytokeratin (AE1/AE3 pancytokeratin), consistent with a sarcoma. In addition, most of the neoplastic cell population demonstrated positive staining for the histiocytic markers major histocompatibility complex (MHC) class II (Figure 6) and ionised calcium binding adaptor molecule 1 (Iba-1) (Figure 7), although a subpopulation of the larger cells appeared to be negative staining for these markers.

A post-mortem USFNA of the lung nodule was also obtained. Cytology documented an abundant population of large immature/atypical individual round cells. The contours were variably well defined and the nucleolus to cytoplasmic ratio was marked. The cells

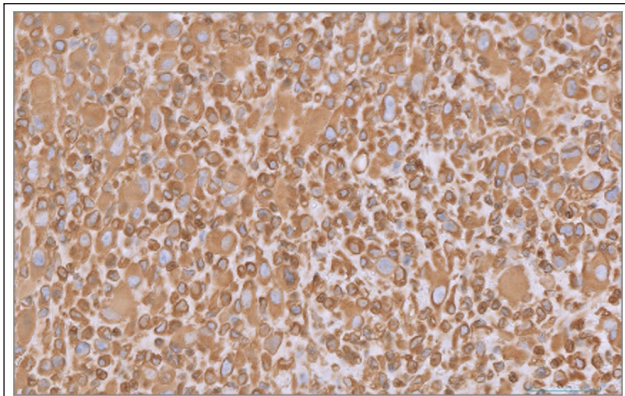


Figure 5 Immunohistochemical staining of the Tru-cut biopsy obtained from the left kidney for the mesenchymal cell marker vimentin. The neoplastic cell population demonstrates strong positive cytoplasmic staining for this marker (brown colouration). Vimentin with haematoxylin counterstain, 400× magnification

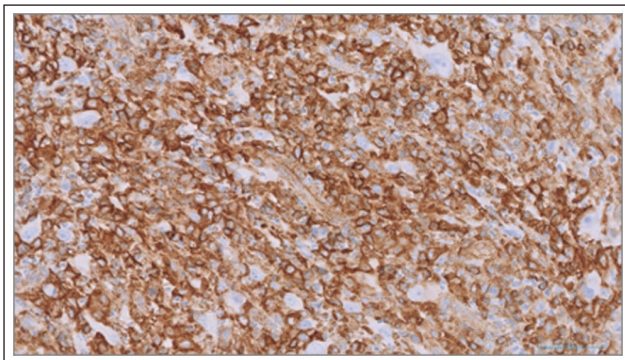


Figure 6 Immunohistochemical staining of the Tru-cut biopsy obtained from the left kidney for the leukocyte marker Major histocompatibility complex class II. The vast majority of the neoplastic cell population demonstrates strong positive staining for this marker (brown colouration). Major histocompatibility complex class II with haematoxylin counterstain, 400× magnification.

measured 15–70 μm and had mildly to moderately abundant cytoplasm, with vacuolisation and features supportive of phagocytosis. The nucleus was oval or rounded and usually paracentral or clearly eccentric. Several cells were bi-, tri- or even multinucleated, with prominent intracellular anisokaryosis. Frequent mitotic figures were visible. Although the exact nature of this cell population remained uncertain, features were most suggestive of HS, like the cells found in kidney. Based on this, lung metastasis from renal HS was considered the most likely diagnosis.

Discussion

Several histiocytic proliferative diseases have been recognised in dogs, but are less frequently described in cats,^{1,2} typically limited to feline progressive histiocyto-

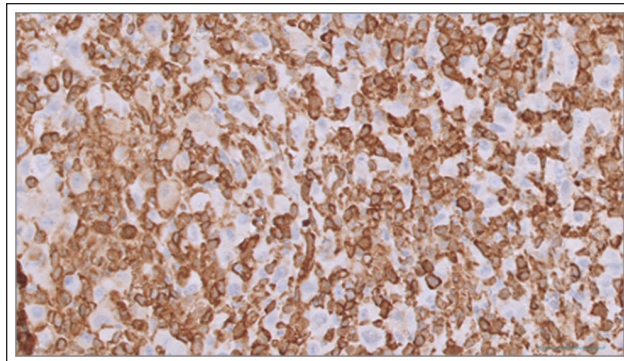


Figure 7 Immunohistochemical staining of the Tru-cut biopsy obtained from the left kidney for the histiocytic marker ionised calcium binding adaptor molecule 1. The majority of the neoplastic cell population demonstrates strong positive staining for this marker (brown colouration); however, a subpopulation of the larger cells appeared to be negative staining. Ionised calcium binding adaptor molecule 1 with haematoxylin counterstain, 400× magnification

sis (FPH), HS and pulmonary Langerhans cell histiocytosis (PLCH).¹

Given the ubiquitous distribution of macrophages or dendritic cells, from which histiocytic disorders originate, HS can arise from almost any tissue.^{1,3} To date, feline HS has been documented in the central nervous system,^{4–7} eyes,⁸ oral and nasal cavities,^{9–11} mediastinum^{12–14} and periarticular space.^{15,16} When present in more than one organ, the primary site of origin is often difficult to ascertain; bone,¹¹ cardiac¹⁶ and renal⁶ metastases have been previously described. Both multicentric disease and a primary tumour with distant metastatic lesions are referred to as disseminated HS,^{1,17} and this is the accepted terminology for what was previously known as malignant histiocytosis (MH).^{18–21} Reports of MH exist, documenting the concurrent involvement of liver, spleen, lungs, kidneys, lymph nodes and bone marrow.²¹

Only limited reports describe HS affecting the kidneys in cats. In two published case reports, renal involvement was assumed to be part of the disseminated disease from primary neoplasms elsewhere.^{6,21} To our knowledge, no case reports have been published describing bilateral primary renal HS in the cat.

Disseminated lung involvement secondary to primary HS is also not explicitly described in the literature, other than in MH.²¹ Other forms of histiocytic disease, such as PLCH, primarily affect the lung²² and frequently have other organ involvement, including lymph nodes, spleen, liver, kidneys, thyroid and parathyroid glands.^{1,2,23} Although the pulmonary nodular opacification documented in the current case can also occur with PLCH,² the absence of documented respiratory insufficiency (the main clinical sign of PLCH)^{2,23} makes PLCH appear unlikely here.

Other studies have previously described the ultrasonographic appearance of HS in dogs²⁴ and in a cat.²⁵ In these studies, hypoechoic irregular nodules with mixed echogenicity and predominantly hypoechoic centres were observed in the liver and spleen of most affected animals, similar to the bilateral nodules found in the renal cortices in the current case. However, such changes have not previously been described in feline renal HS. In this case, the remaining findings were similar to those commonly seen in renal lymphoma (eg, diffuse echogenicity changes, bilateral renal enlargement, distortion of the kidney contour and hypoechoic subcapsular thickening),²⁶ the most common renal neoplasm in cats.^{17,27} Therefore, HS should be considered a differential diagnosis when renal lymphoma is suspected based on ultrasonographic features, particularly when hypoechoic nodules are also identified within the renal cortex.

A definitive diagnosis of HS requires morphological and immunohistochemical confirmation of the histiocytic lineage.⁶ In this case, the immunohistochemical staining pattern of the neoplastic cells was consistent with a sarcoma, with positive staining for the non-specific mesenchymal cell marker vimentin. There was also positive staining of most of the neoplastic cell population with histiocytic markers Iba-1 (macrophage/monocyte lineage) and MHC II (antigen-presenting cells), supportive of a histiocytic origin.^{8,14,28} The diagnosis of HS was based on both gross findings and cytological/histopathological features. Nevertheless, a small subpopulation of larger neoplastic cells displayed negative staining, and the possibility of other forms of sarcoma, in particular an undifferentiated pleomorphic sarcoma (previously known as anaplastic sarcoma with giant cells),²⁹ could not be completely excluded.

When HS presents in more than one organ, the primary origin of the cancerous process is often difficult to ascertain. In this case, neither full-body diagnostic imaging nor post-mortem examination were performed; therefore, the presence of histiocytic disease in other organs could not be definitively excluded. Nevertheless, with the available information, we strongly suspect the HS was renal in origin, given the notable ultrasonographic changes and supportive histopathological and immunohistochemical findings. The lung nodules were suspected to be a result of disseminated disease.

The prognosis for cats with HS is poor, and data on treatment options and response are limited.^{14,30,31} More information exists on the treatment of HS in dogs.^{30,31} In humans, HS also carries a poor prognosis, with most patients dying of progressive disease within 1 year of diagnosis.³² Increasing awareness of feline HS should prompt further studies, which will hopefully provide treatment options and prognostic information.

Conclusions


This is the first reported case of a cat with bilateral renal HS with pulmonary metastasis. A primary renal origin was suspected, with the lung lesions likely a result of disseminated disease. To our knowledge, while a few reports describe HS with renal involvement in cats, this is the first case in which the kidneys were considered to be the primary origin. Renal HS should be included as a differential diagnosis when renal ultrasound reveals changes suggestive of neoplasia.

Conflict of interest The authors declared no potential conflicts of interest with respect to the research, authorship, and/or publication of this article.

Funding The authors disclosed receipt of the following financial support for the research, authorship, and/or publication of this article: Financial support was received from CVS group for the post-mortem cytological and histopathological examination of the tissues of interest (kidneys and lungs).

Ethical approval The work described in this manuscript involves the use of non-experimental (owned or unowned) animals. Established internationally recognised high standards ('best practice') of veterinary clinical care for the individual patient were always followed and/or this work involved the use of cadavers. Ethical approval from a committee was therefore not specifically required for publication in *JFMS Open Reports*. Although not required, where ethical approval was still obtained, it is stated in the manuscript.

Informed consent Informed consent (verbal or written) was obtained from the owner or legal custodian of all animal(s) described in this work (experimental or non-experimental animals, including cadavers) for all procedure(s) undertaken (prospective or retrospective studies). No animals or people are identifiable within this publication, and therefore additional informed consent for publication was not required.

ORCID ID Melanie Dobromylskij  <https://orcid.org/0000-0002-0781-5726>

References

- 1 Moore PF. **A review of histiocytic diseases of dogs and cats.** *Vet Pathol* 2014; 51: 167–184.
- 2 Argenta FF, de Britto FC, Pereira PR, et al. **Pulmonary Langerhans cell histiocytosis in cats and a literature review of feline histiocytic diseases.** *J Feline Med Surg* 2020; 22: 305–312.
- 3 Hirabayashi M, Chambers JK, Sumi A, et al. **Immunophenotyping of nonneoplastic and neoplastic histiocytes in cats and characterization of a novel cell line derived from feline progressive histiocytosis.** *Vet Pathol* 2020; 57: 758–773.
- 4 Vernau KM, Higgins RJ, Bollen AW, et al. **Primary canine and feline nervous system tumors: intraoperative diagnosis using the smear technique.** *Vet Pathol* 2001; 38: 47–57.

- 5 Ide T, Uchida K, Tamura S, et al. **Histiocytic sarcoma in the brain of a cat.** *J Vet Med Sci* 2010; 72: 99–102.
- 6 Monteiro S, Hughes K, Genain MA, et al. **Primary histiocytic sarcoma in the brain with renal metastasis causing internal ophthalmoparesis and external ophthalmoplegia in a Maine Coon cat.** *JFMS Open Rep* 2021; 7. DOI: 10.1177/20551169211038515.
- 7 Riker J, Clarke LL, Demeter EA, et al. **Histiocytic sarcoma with central nervous system involvement in 6 cats.** *J Vet Diagn Invest* 2023; 35: 87–91.
- 8 Scurrall E, Trott A, Rozmanec M, et al. **Ocular histiocytic sarcoma in a cat.** *Vet Ophthalmol* 2013; 16 Suppl 1: 173–176.
- 9 Santifort KM, Jurgens B, Grinwis GC, et al. **Invasive nasal histiocytic sarcoma as a cause of temporal lobe epilepsy in a cat.** *JFMS Open Rep* 2018; 4. DOI: 10.1177/2055116918811179.
- 10 Néčová S, North S, Cahalan S, et al. **Oral histiocytic sarcoma in a cat.** *JFMS Open Rep* 2020; 6. DOI: 10.1177/2055116920971248.
- 11 Ruppert SL, Ferguson SH, Struthers JD, et al. **Oral histiocytic sarcoma in a cat with mandibular invasion and regional lymph node metastasis.** *JFMS Open Rep* 2021; 7. DOI: 10.1177/20551169211058044.
- 12 Walton RM, Brown DE, Burkhard MJ, et al. **Malignant histiocytosis in a domestic cat: cytomorphologic and immunohistochemical features.** *Vet Clin Pathol* 1997; 26: 56–60.
- 13 Smoliga J, Schatzberg S, Peters J, et al. **Myelopathy caused by a histiocytic sarcoma in a cat.** *J Small Anim Pract* 2005; 46: 34–38.
- 14 Bisson J, Van den Steen N, Hawkins I, et al. **Mediastinal histiocytic sarcoma with abdominal metastasis in a Somali cat.** *Vet Rec Case Rep* 2017; 5. <https://doi.org/10.1136/vet-reccr-2016-000405>.
- 15 Pinard J, Wagg CR, Girard C, et al. **Histiocytic sarcoma in the tarsus of a cat.** *Vet Pathol* 2006; 43: 1014–1017.
- 16 Chalfon C, Romito G, Sabattini S, et al. **Periarticular histiocytic sarcoma with heart metastasis in a cat.** *Vet Clin Pathol* 2021; 50: 579–583.
- 17 Williams AG, Hohenhaus AE and Lamb KE. **Incidence and treatment of feline renal lymphoma: 27 cases.** *J Feline Med Surg* 2021; 23: 936–944.
- 18 Moore PF and Rosin A. **Malignant histiocytosis of Bernese mountain dogs.** *Vet Pathol* 1986; 23: 1–10.
- 19 Freeman L, Stevens J, Loughman C, et al. **Clinical vignette.** *J Vet Intern Med* 1995; 9: 171–173.
- 20 Favara BE, Feller AC, Pauli M, et al. **Contemporary classification of histiocytic disorders. The WHO Committee on Histiocytic/Reticulum Cell Proliferations. Reclassification Working Group of the Histiocyte Society.** *Med Pediatr Oncol* 1997; 29: 157–166.
- 21 Kraje AC, Patton CS and Edwards DF. **Malignant histiocytosis in 3 cats.** *J Vet Intern Med* 2001; 15: 252–256.
- 22 Vail DM, Thamm DH and Liptak JM (eds). **Withrow and MacEwen's small animal clinical oncology.** Vol. I. 6th ed. St. Louis, MO: Elsevier, 2019.
- 23 Busch MDM, Reilly CM, Luff JA, et al. **Feline pulmonary Langerhans cell histiocytosis with multiorgan involvement.** *Vet Pathol* 2008; 45: 816–824.
- 24 Huber B and Leleonnec M. **Diagnosis and treatment of hemophagocytic histiocytic sarcoma in a cat.** *JFMS Open Rep* 2020; 6. DOI: 10.1177/2055116920957196.
- 25 Cruz-Arámbulo R, Wrigley R and Powers B. **Sonographic features of histiocytic neoplasms in the canine abdomen.** *Vet Radiol Ultrasound* 2004; 45: 554–558.
- 26 Valdés-Martínez A, Cianciolo R and Mai W. **Association between renal hypoechoic subcapsular thickening and lymphosarcoma in cats.** *Vet Radiol Ultrasound* 2007; 48: 357–360.
- 27 Mooney SC, Hayes AA, Matus RE, et al. **Renal lymphoma in cats: 28 cases (1977-1984).** *J Am Vet Med Assoc* 1987; 191: 1473–1477.
- 28 Teshima T, Hata T, Nezu Y, et al. **Amputation for histiocytic sarcoma in a cat.** *J Feline Med Surg* 2012; 14: 147–150.
- 29 de Cecco BS, Argenta FF, Bianchi RM, et al. **Feline giant-cell pleomorphic sarcoma: cytologic, histologic and immunohistochemical characterization.** *J Feline Med Surg* 2021; 23: 738–744.
- 30 Rassnick KM, Moore AS, Russell DS, et al. **Phase II, open-label trial of single-agent CCNU in dogs with previously untreated histiocytic sarcoma.** *J Vet Intern Med* 2010; 24: 1528–1531.
- 31 Cannon C, Borgatti A, Henson M, et al. **Evaluation of a combination chemotherapy protocol including lomustine and doxorubicin in canine histiocytic sarcoma.** *J Small Anim Pract* 2015; 56: 425–429.
- 32 Tocut M, Vaknine H, Potachenko P, et al. **Histiocytic sarcoma.** *Isr Med Assoc J* 2020; 22: 645–647.